

# **LEGIBILITY NOTICE**

**A major purpose of the Technical Information Center is to provide the broadest dissemination possible of information contained in DOE's Research and Development Reports to business, industry, the academic community, and federal, state and local governments.**

**Although a small portion of this report is not reproducible, it is being made available to expedite the availability of information on the research discussed herein.**

LA-UR--89-1462

Received

11

CONF-890771--2

MAY 09 1989

Los Alamos National Laboratory is operated by the University of California for the United States Department of Energy under contract W-7405-ENG-36

LA-UR--89-1462

DE89 011164

**TITLE: MODELING OF NON-STRUCTURAL CONTRIBUTION TO THE PATTERN**

**AUTHOR(s): Robert B. Von Dreele, LANSCE**

**SUBMITTED TO: Invited Conference Presentation; ACA Rietveld Workshop,  
July 28, 1989, Seattle, Washington**

**DISCLAIMER**

This report was prepared as an account of work sponsored by an agency of the United States Government. Neither the United States Government nor any agency thereof, nor any of their employees, makes any warranty, express or implied, or assumes any legal liability or responsibility for the accuracy, completeness, or usefulness of any information, apparatus, product, or process disclosed, or represents that its use would not infringe privately owned rights. Reference herein to any specific commercial product, process, or service by trade name, trademark, manufacturer, or otherwise does not necessarily constitute or imply its endorsement, recommendation, or favoring by the United States Government or any agency thereof. The views and opinions of authors expressed herein do not necessarily state or reflect those of the United States Government or any agency thereof.

By acceptance of this article, the publisher recognizes that the U.S. Government retains a nonexclusive, royalty-free license to publish or reproduce the published form of this contribution, or to allow others to do so, for U.S. Government purposes.

The Los Alamos National Laboratory requests the publisher identify this article as work performed under the auspices of the U.S. Department of Energy.

Los Alamos

Los Alamos National Laboratory  
Los Alamos, New Mexico 87545

## MODELING OF NON-STRUCTURAL CONTRIBUTION TO THE PATTERN

Robert B. Von Dreele  
Manuel Lujan Jr., Neutron Scattering Center (LANSCE), MS H805  
Los Alamos National Laboratory, Los Alamos, NM 87545

### ABSTRACT

The Rietveld refinement technique requires that sensible models be chosen for both the Bragg reflection profiles and intensities as well as the background contribution. The reflection profiles contain an instrumental part and a sample dependent part that is affected by particle size and strain. The intensities are affected by geometric factors peculiar to the diffraction method and sample dependent effects such as absorption, extinction and preferred orientation. The various functions used for these effects in Rietveld refinement will be discussed along with the possible interpretation of their coefficients.

### RIETVELD REFINEMENT

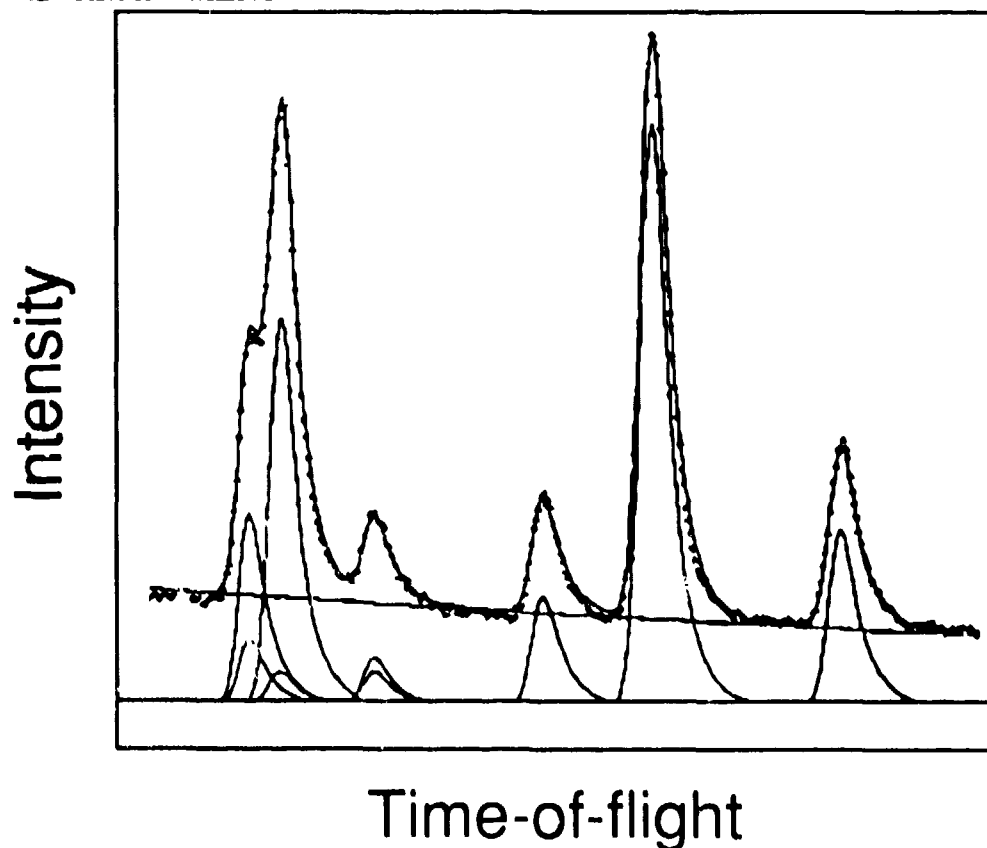


Figure 1. A portion of a TOF neutron powder diffraction pattern showing the individual contributions to the total profile intensity. Nine diffraction peaks and a background curve are shown along with their sum as lines and the observed profile as crosses.

About 20 years ago, H.M. Rietveld (1969) recognized that a mathematical expression could be written to represent the observed intensity at every step in a neutron powder diffraction pattern.

$$I_c = I_b + \sum Y_h \quad (1)$$

This expression has both a contribution from the background ( $I_b$ ) and each of the Bragg reflections ( $Y_h$ ) which are in the vicinity of the powder pattern step (Figure 1).

Each of these components to the intensity is represented by a mathematical model which embodies both the crystalline and noncrystalline features of a powder diffraction experiment. The adjustable parameters for this model are refined by a least-squares minimization of the weighted differences between the observed and calculated intensities. This approach to the analysis of powder patterns has been so successful that it has led to a renaissance in powder diffraction and this technique of treating powder diffraction data is now known as "Rietveld refinement." This article will discuss only the Bragg component of the intensity; the background models will be discussed in another talk in this Workshop.

## BRAGG INTENSITY

The contributed intensity,  $Y_h(T)$ , from a Bragg peak to a particular profile intensity will depend on several factors. Obviously the value of the structure factor and the amount of that particular phase will determine the contribution. In addition, the peak shape and width in relation to its position will have an effect. The intensity is also affected by extinction and absorption as well as some geometric factors. Thus,

$$Y_h(T) = SF_h^2 H(T-T_h) K_h \quad (2)$$

where  $S$  is the scale factor for the particular phase,  $F_h$  is the structure factor for a particular reflection,  $H(T-T_h)$  is the value of the profile peak shape function for that reflection at the position,  $T$ , which is displaced from its expected position,  $T_h$ , and  $K_h$  is the product of the various geometric and other correction factors for that reflection. Each of these contributions will be

## PROFILE FUNCTIONS FOR CW AND TOF

The contribution a given reflection makes to the total profile intensity depends on the shape function for that reflection profile, its width coefficients and the displacement of the peak from the profile position. The locations of the peak are usually given in microseconds of TOF or in centidegrees  $2\Theta$ . Discussion of these values is given first followed by details of some of the peak shape functions presently in use.

## REFLECTION POSITIONS IN POWDER PATTERNS

For a neutron time-of-flight powder diffractometer the relationship between the d-spacing for a particular powder line and its TOF is given by the simple quadratic

$$T_h = C d_h + A d_h^2 + Z \quad (3)$$

The three parameters C, A and Z are characteristic of a given counter bank on a TOF powder diffractometer. C may be calculated with good precision from the flight paths, diffraction angle, and counter tube length by use of the de Broglie equation.

$$C = 252.816 * 2 \sin \Theta (L_1 + \sqrt{L_2^2 + L_3^2 / 16}) \quad (4)$$

where  $\Theta$  is the Bragg angle,  $L_1$  is the primary flight path,  $L_2$  is sample to detector center distance and  $L_3$  is the height of the detector; all distances are in meters. The units of C are then  $\mu\text{sec}/\text{\AA}$ . Precise values for constants C, A and Z must be obtained by fitting to a powder diffraction pattern of a standard material.

The reflection position in a constant wavelength experiment is obtained from Bragg's Law

$$T_h = 100 a \sin(\lambda / 2d_h) + Z \quad (5)$$

where Z is the zero point error on the counter arm position and the result is in centidegrees. Both  $\lambda$  and Z for neutrons or synchrotron x-rays are obtained from refinement of a standard material. For conventional sealed tube x-ray sources on a commercial instrument, the wavelength is known to high accuracy and careful instrument alignment yields Z of zero.

## TOF PROFILE FUNCTIONS

The best known profile function for TOF neutron data is the empirical convolution function of Jorgensen et al. (1978) and Von Dreele, et al. (1982).

$$H(\Delta T) = N[e^u \operatorname{erfc}(y) + e^v \operatorname{erfc}(z)] \quad (6)$$

where  $\Delta T$  is the difference in TOF between the reflection position,  $T_h$ , and the profile point,  $T$ ; the terms  $N, u, v, y$  and  $z$  are dependent on the profile coefficients. The function  $\operatorname{erfc}(x)$  is the complementary error function. This profile function is the result of convoluting two back-to-back exponentials with a Gaussian.

$$H(\Delta T) = \int G(\Delta T - \tau) P(\tau) d\tau \quad (7)$$

where

$$P(\tau) = 2Ne^{\alpha\tau} \text{ for } \tau < 0 \quad (8)$$

and

$$P(\tau) = 2Ne^{-\beta\tau} \text{ for } \tau > 0 \quad (9)$$

for the two exponentials;  $\alpha$  and  $\beta$  are the rise and decay coefficients for the exponentials and are largely characteristic of the specific moderator viewed by the instrument. The intersection of the two exponentials at  $\tau=0$  then defines the peak location,  $T_h$ , which is generally not coincident with the maximum in  $H(\Delta T)$ . The Gaussian function is

$$G(\Delta T - \tau) = \frac{1}{\sqrt{2\pi\sigma^2}} e^{-(\Delta T - \tau)^2/2\sigma^2} \quad (10)$$

where the variance,  $\sigma^2$ , is largely characteristic of the instrument design (scattering angle and flight path) and the sample. These functions when convoluted give the profile function shown above. The normalization factor,  $N$ , is

$$N = \frac{\alpha\beta}{2(\alpha + \beta)} \quad (11)$$

The coefficients  $u, v, y$  and  $z$  are

$$u = \frac{\alpha}{2}(\alpha\sigma^2 + 2\Delta T) \quad (12)$$

$$v = \frac{\beta}{2}(\beta\sigma^2 - 2\Delta T) \quad (13)$$

$$y = \frac{(\alpha\sigma^2 + \Delta T)}{\sqrt{2\sigma^2}} \quad (14)$$

$$z = \frac{(\beta\sigma^2 - \Delta T)}{\sqrt{2\sigma^2}} \quad (15)$$

Each of the three coefficients  $\alpha$ ,  $\beta$  and  $\sigma^2$  all show a specific empirical dependence on the reflection d-spacing.

$$\alpha = \alpha_0 + \alpha_1/d \quad (16)$$

$$\beta = \beta_0 + \beta_1/d^4 \quad (17)$$

$$\sigma^2 = \sigma_0^2 + \sigma_1^2 d^2 + \sigma_2^2 d^4 \quad (18)$$

The last expression is a sum of variances with contributions from the instrument and from strain and particle size broadening by the sample.

## INTERPRETATION OF TOF PROFILE COEFFICIENTS

The profile coefficients from a time of flight (TOF) neutron powder pattern Rietveld refinement can give information about the microtexture of the sample. This discussion will describe how this information can be extracted from the coefficients.

The strain in a lattice can be visualized as a distribution of unit cell dimensions about the average lattice parameters induced by defects. In the reciprocal space (Figure 2) associated with a sample with isotropic strain, there is a broadening of each point which is proportional to the

$$\frac{\Delta d^*}{d^*} = \text{constant} \quad (19)$$

In real space (the regime of a TOF experiment) then

$$\frac{\Delta d}{d} = \text{constant} \quad (20)$$

for strain broadening. Thus, examination of the function for the Gaussian component of the peak shape from a TOF pattern (Equation 18) implies that the second term contains an isotropic contribution from: strain broadening. The other major contribution to  $\sigma_1^2$  is from the instrument; and because it is expressed as a variance, it can simply be subtracted. The remaining sample dependent contribution is then converted to strain (S), a dimensionless value which is frequently expressed as percent strain or fractional strain as a full width at half maximum.

$$S = 100\% \frac{1}{C} \sqrt{2 \ln 2 (\sigma_1^2 - \sigma_{i1}^2)} \quad (21)$$

where C is the diffractometer constant from Equation 3.

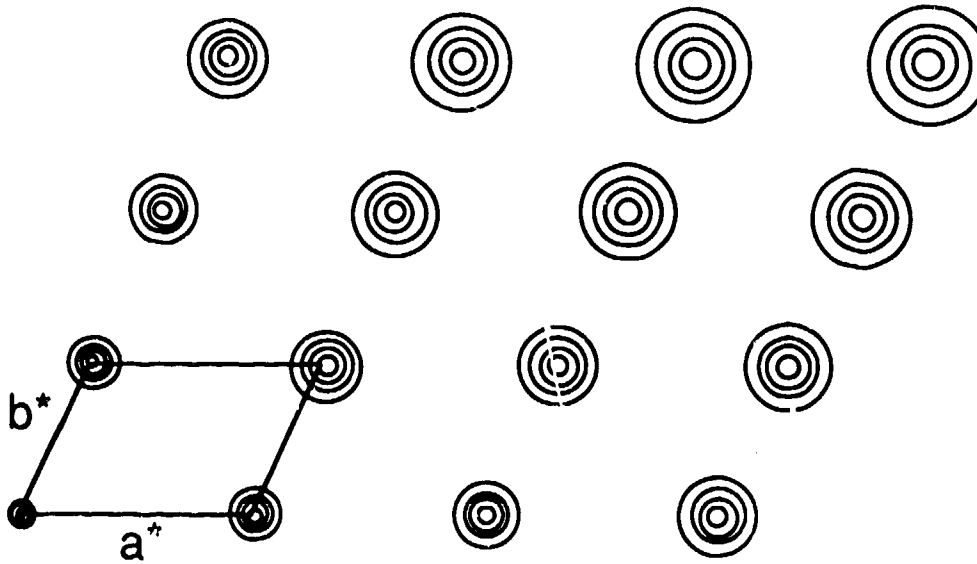


Figure 2. The broadening of reciprocal lattice points due to strain.

For small particles the assumption that the lattice is infinite no longer holds so that the reciprocal lattice points,  $\mathbf{h}$ , are not  $\delta$ -functions but are smeared out uniformly depending on the average particle size. Thus, all the points are the same size independent of the distance from the origin (Figure 3)



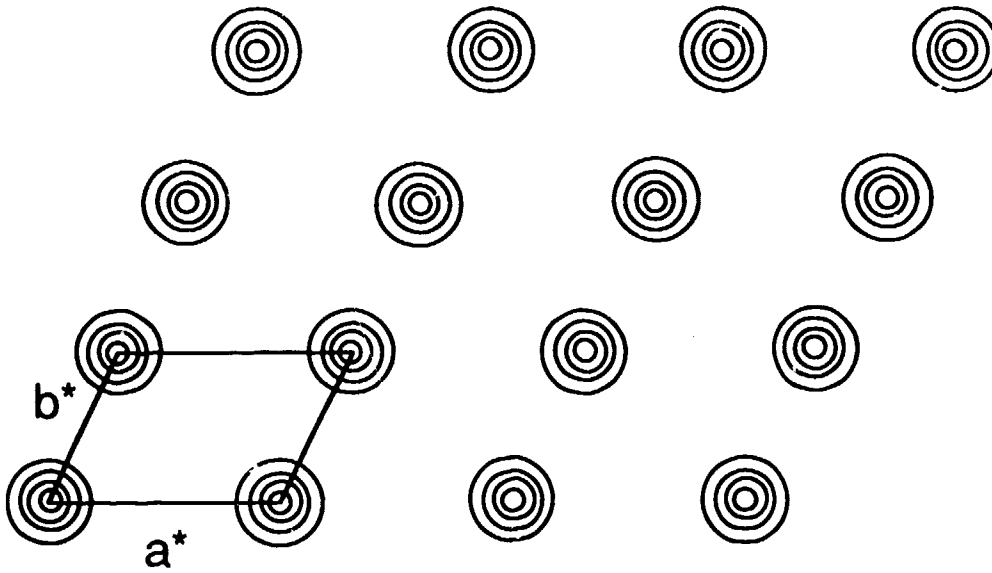


Figure 3. The broadening in reciprocal space due to particle size.

and

$$\Delta d^* = \text{constant} \quad (22)$$

The reciprocal of this quantity is the average particle size. In real space (for TOF) the broadening is

$$\frac{\Delta d}{d^2} = \text{constant} \quad (23)$$

From the functional form for the Gaussian broadening of a TOF peak (Equation 18), the particle size affects the third term ( $\sigma_2^2$ ) in the expression. This term generally has no instrument contribution and is used directly to calculate the particle size ( $p$ ) by

$$p = \frac{2C}{\sqrt{2 \ln 2} \sigma_2} \quad (24)$$

where  $C$  is the diffractometer constant and the units for  $p$  are  $\text{\AA}$ .

## CW PROFILE FUNCTIONS

The most successful function for both x-ray and neutron CW data employs a multi-term Simpson's rule integration described by Howard (1982) of the pseudo-Voigt,  $F(\Delta T)$ , described by Thompson, et al. (1987).

$$H(\Delta T) = \sum_{i=1}^n g_i F(\Delta T^i) \quad (25)$$

where the pseudo-Voigt is

$$F(\Delta T) = \eta L(\Delta T, \Gamma) + (1-\eta)G(\Delta T, \Gamma) \quad (26)$$

and the Lorentzian function is

$$L(\tau) = \frac{\gamma}{2\pi} \left[ \frac{1}{(\gamma/2)^2 + \tau^2} \right] \quad (27)$$

The Gaussian expression is the same as used for the TOF function above (Equation 10). The mixing factor,  $\eta$ , is given by

$$\eta = 1.36603(\gamma/\Gamma) - 0.47719(\gamma/\Gamma)^2 + 0.11116(\gamma/\Gamma)^3 \quad (28)$$

and the FWHM parameter is

$$\Gamma = \sqrt[5]{\Gamma_g^5 + 2.69269\Gamma_g^4\gamma + 2.42843\Gamma_g^3\gamma^2 + 4.47163\Gamma_g^2\gamma^3 + 0.07842\Gamma_g\gamma^4 + \gamma^5} \quad (29)$$

where the Gaussian FWHM is

$$\Gamma_g = 2\sqrt{2\ln 2}\sigma^2 \quad (30)$$

The  $2\Theta$  difference modified for asymmetry,  $A_s$ , and sample shift,  $S_s$ , is

$$\Delta T^i = \Delta T + \frac{f_i A_s}{\tan 2\Theta} + S_s \cos \Theta \quad (31)$$

where the sums have 3, 5 or 7 terms depending on the size of  $A_s$ . The corresponding Simpson's rule coefficients,  $g_i$  and  $f_i$ , depend on the number of terms in the summation. The sample shift can be interpreted as a physical shift of the sample,  $s$ , from the diffractometer axis by

$$s = \frac{-\pi R S_s}{36000} \quad (32)$$

where  $R$  is the diffractometer radius. This sample shift is usually only observed for measurements done on conventional instruments with focussing geometry. The variance of the peak,  $\sigma^2$ , varies with  $2\Theta$  as

$$\sigma^2 = U \tan^2 \Theta + V \tan \Theta + W + \frac{P}{\cos^2 \Theta} \quad (33)$$

where  $U$ ,  $V$  and  $W$  are the coefficients described by Cagliotti et al. (1958) and  $P$  is the Scherrer coefficient for Gaussian broadening. The Lorentzian coefficient,  $\gamma$ , varies as

$$\gamma = \frac{X}{\cos \Theta} + Y \tan \Theta + Z \quad (34)$$

The first term is the Lorentzian Scherrer broadening and the second term describes strain broadening.

## INTERPRETATION OF CW PROFILE COEFFICIENTS

In the case of a CW experiment the strain broadening in real space is related to  $2\Theta$  broadening from

$$\frac{\Delta d}{d} = \Delta 2\Theta \cot \Theta = \text{constant} \quad (35)$$

or

$$\Delta 2\Theta = \frac{\Delta d}{d} \tan \Theta \quad (36)$$

In this expression  $\Delta 2\Theta$  is in radians. Examination of the expression for the Gaussian broadening (Equation 33) indicates that the first term contains a strain broadening component. As for the

TOF expression, this is a variance and the instrument contribution can be subtracted. This variance must be converted to radians to yield strain, thus

$$S = 100\% \frac{\pi}{9000} \sqrt{2 \ln 2 (U - U_i)} \quad (37)$$

Alternatively, the strain term is the one that varies with  $\tan \Theta$  in the Lorentzian component of a CW peak shape (Equation 34). Again any instrumental or spectral contribution can be subtracted to yield the strain component. This is in cdeg and is already a full width at half maximum so the strain is

$$S = 100\% \frac{\pi}{18000} (Y - Y_i) \quad (38)$$

For the case of a CW experiment the particle size broadening can be obtained from

$$\frac{\Delta d}{d^2} = \frac{\Delta 2\Theta}{d} \cot \Theta = \text{constant} \quad (39)$$

From Bragg's law then

$$\frac{\Delta d}{d^2} = \frac{2\Delta 2\Theta}{\lambda} \cot \Theta \sin \Theta \quad (40)$$

and the broadening is

$$\Delta 2\Theta = \frac{\lambda \Delta d}{2d \cos \Theta} \quad (41)$$

The first term in the expression for the Lorentzian broadening is of this form where

$$X = \frac{1}{2} \frac{\Delta d}{d} \quad (42)$$

The particle size can be obtained by rearrangement of this expression and converting from centidegrees to radians by

$$p = \frac{9000\lambda}{\pi X} \quad (43)$$

The units are Å.

The corresponding term in the Gaussian expression is the fourth one. Converting from centidegrees to radians gives the expression

$$P = \frac{4500\lambda}{\pi\sqrt{2\ln 2}P} \quad (44)$$

and again the units are Å.

## SYSTEMATIC EFFECTS ON THE INTENSITY

The intensity correction factors,  $K_h$ , consist of those factors which are dependent on the sample, the instrument geometry, and the type of radiation used.

$$K_h = \frac{E_h A_h O_h M_h L}{V_h} \quad (45)$$

where  $E_h$  is an extinction correction,  $A_h$  is an absorption correction,  $O_h$  is the preferred orientation correction,  $M_h$  is the reflection multiplicity,  $L$  is the angle dependent Lorentz and polarization correction, and  $V_h$  is the unit cell volume for the phase. Some of them will be discussed in turn.

## EXTINCTION IN POWDERS

The extinction in powders is calculated according to a formalism developed by Sabine, Von Dreele and Jorgensen (1985 & 1988) and is a primary extinction effect within the crystal grains. From the Darwin (1922) energy transfer equations Sabine (1988), by following the formalisms of Zachariasen (1945, 1967) and Hamilton (1957), developed intensity expressions for both the symmetric Laue and Bragg cases of diffraction by an infinite plane parallel plate. The extinction correction  $E_h$  for a small crystal is a combination of Bragg and Laue components

$$E_h = E_b \sin^2(\theta) + E_l \cos^2(\theta) \quad (46)$$

where

$$E_b = 1/\sqrt{1+x} \quad (47)$$

and

$$E_l = 1 - \frac{x}{2} + \frac{x^2}{4} - \frac{5x^3}{48} \dots \text{ for } x < 1 \quad (48)$$

or

$$E_l = \sqrt{\frac{2}{\pi x}} \left[ 1 - \frac{1}{8x} - \frac{3}{128x^2} \dots \right] \text{ for } x > 1 \quad (49)$$

where

$$x = E_x(\lambda F_h/V)^2, \quad (50)$$

$F_h$  is the calculated structure factor and  $V$  is the unit cell volume. The units for these expressions are such that  $E_x$  is in  $\mu\text{m}^2$  and is a direct measure of the block size in the powder sample. Sabine et al. (1988) demonstrated this by examining the extinction effects for neutron powder diffraction by hot pressed MgO samples characterized by electron microscopy; the refined extinction coefficients correlated very well with the measured particle size distribution in these samples.

## POWDER ABSORPTION FACTOR

The absorption,  $A_h$ , for a cylindrical sample is calculated for neutron powder data according to an empirical formula (Hewat, 1979 and Rouse et al. 1970). It is assumed that the linear absorption of all components in the sample vary with  $\lambda$  and is indistinguishable from multiple scattering effects within the sample.

$$A_h = e \cdot (T_1 \Lambda_B \lambda + T_2 \Lambda_B^2 \lambda^2) \quad (51)$$

where

$$T_1 = 1.7133 - 0.368 \sin^2 \Theta \quad (52)$$

and

$$T_2 = -0.0927 - 0.3750 \sin^2 \Theta \quad (53)$$

For a fixed wavelength, this expression is indistinguishable from thermal motion effects and hence cannot be refined independently of atomic thermal parameters.

X-ray diffraction data is usually taken with a flat plate sample where the macroscopic absorption is a constant independent of scattering angle. There has been observed some microabsorption effects particularly when multiphase mixtures are examined. If the components of the mixture have very different absorption coefficients then the relative scale factors frequently do not reflect the

### PREFERRED ORIENTATION OF POWDERS

The preferred orientation correction,  $O_h$ , is the formulation of Dollase (1986) who selected a special case from the more general description by March (1932). For this model, the crystallites are assumed to be effectively either rod or disk shaped. When the powder is packed into either a flat plate or a cylinder, the crystallite axes will take up a preferred orientation that can be described with a cylindrically symmetric ellipsoidal distribution function. In the usual diffraction geometries for powder diffraction the unique axis of this distribution is either normal to the diffraction plane or along the diffraction vector ( $\mathbf{h}$ ), and integration about this distribution at the scattering angle for each reflection gives a very simple form for the correction,

$$O_h = \sum_{j=1}^n (R_0^2 \cos^2 A_j + \sin^2 A_j / R_0)^{-3/2} / M \quad (54)$$

where  $A_j$  is the angle between the preferred orientation direction and the reflection vector  $\mathbf{h}$ . The sum is over the reflections equivalent to  $\mathbf{h}$ . The one refineable coefficient,  $R_0$ , is the axis ratio for the ellipsoid and gives the effective sample compression or extension due to preferred orientation. If there is no preferred orientation then the distribution is spherical and  $R_0 = 1.0$  and thus  $O_h = 1.0$ .

## OTHER ANGLE DEPENDENT CORRECTIONS

The only other angle dependent correction for powder diffraction data is the Lorentz and x-ray polarization factors. For TOF neutron data there is an additional factor for the variation of scattered intensity with wavelength thus

$$L = d^4 \sin \Theta \quad (55)$$

and for constant wavelength neutrons

$$L = \frac{1}{2 \sin 2\Theta \cos \Theta} \quad (56)$$

For conventional X-ray sources there is a polarization effect which depends on the choice and orientation of the monochromator (Azaroff, 1955). X-rays emitted from synchrotron sources are very strongly polarized which dramatically modifies the scattered intensities of a powder pattern. All these effects can be combined in a single expression

$$L = \frac{P_h + (1 - P_h) \cos^2 \Theta}{2 \sin^2 \Theta \cos \Theta} \quad (57)$$

The coefficient  $P_h$  depends on the polarization of the incident beam; for synchrotron radiation  $P_h \approx 0.95$  while for conventional sources with a crystal monochromator usually  $P_h \approx 0.7$ . If no monochromator is used then  $P_h = 0.5$ .

## REFERENCES

- Azaroff, L.V. (1955). *Acta Cryst.* **8**, 701-704.  
 Cagliotti, G., Paoletti, A. & Ricci, F.P. (1958). *Nucl. Inst.* **3**, 223.  
 Darwin, C.G. (1922). *Philos. Mag.* **43**, 800-829.  
 Dollase, W.A. (1986). *J. Appl. Cryst.* **19**, 267-272.  
 Hamilton, W.C. (1957). *Acta Cryst.* **10**, 620-34.  
 Hewat, A.W. (1979). *Acta Cryst.* **A35**, 248.  
 Howard, C.J. (1982). *J. Appl. Cryst.* **15**, 615-620.



- Jorgensen, J.D., Johnson, D.H., Mueller, M.H., Worlton, J.G. & Von Dreele, R.B. (1978). Proc. Conf. on Diffraction Profile Analysis, Cracow, 14-15 Aug., 20-22.
- March, A. (1932). Z. Kristallogr. **81**, 285-297.
- Rietveld, H.M. (1969). J. Appl. Cryst. **2**, 65-71.
- Rouse, K.D., Cooper, M.J. & Chakera, A. (1970). Acta Cryst. **A26**, 682-691.
- Sabine, T.M. (1985). Aust. J. Phys. **38**, 507-18.
- Sabine, T.M. (1988). Acta Cryst. **A44**, 368-373.
- Sabine, T.M., Von Dreele, R.B. & Jørgensen, J.-E. (1988). Acta Cryst **A44**, 374-379.
- Thompson, P., Cox, D.E. & Hastings, J.B. (1987). J. Appl. Cryst. **20**, 79-83.
- Von Dreele, R.B., Jorgensen, J.D. & Windsor, C.G. (1982). J. Appl. Cryst. **15**, 581-589.
- Zacharaisen, W.H. (1945). "Theory of X-ray Diffraction in Crystals" (Wiley:New York).
- Zacharaisen, W.H. (1967). Acta Cryst. **23**, 558-64.